Final Report
to
Crucible Ventures
on

Evaluation of Thermogalvanic Cells for the Conversion of Heat to Electricity

Jefferson W. Tester, Principal Investigator
Ulrich Holeschovsky
Kersten C. Link
Jay Corbett

Department of Chemical Engineering and
Energy Laboratory
Massachusetts Institute of Technology
Cambridge, Massachusetts
MIT-EL 92-007

November 15, 1992

Table of Contents

Evaluation of Thermogalvanic Cells for the Conversion of Heat to Electricity

1. INTRODUCTION

Conventional power generation and many other industrial processes generate heat as a byproduct. Since this residual thermal energy can only be converted into electricity at very low efficiencies, it is typically released to the environment by means of cooling towers. Thermogalvanic heat conversion, as studied in this report, however, has the potential to produce electricity from such low grade waste heat.

The first experiments on thermogalvanic cells, made over a century ago, were inspired by the analogy between such cells and metallic thermocouples (thermoelectric devices). In recent years, developments in the thermodynamics of irreversible processes have directed attention to nonisothermal systems in general. However, the relatively poor showing of ionic systems due to their high internal resistances [1] has kept research of such systems in an experimental stage. The possibility of using thermogalvanic cells with fused or solid-salt electrolytes as high-temperature thermoelectric generators has been discussed by Christy [2] and Sundheim [3]. However, the conversion of low grade heat into electricity involves temperatures in the range of 20 - 100°C. Aqueous electrolytes are suitable for this temperature range.

In this project, we were interested in analyzing the performance of thermogalvanic cells to evaluate whether industrially competitive efficiencies could be achieved. This effort was motivated by results obtained by Robert Peck. While our work was principally concerned with the independent evaluation of thermogalvanic cells, we also tried to reproduce some of Peck's experiments summarized in his patents [4] and [5].

2. THEORETICAL ASPECTS

2.1 EMF OF A THERMOGALVANIC CELL

Thermogalvanic cells are electrochemical cells in which energy is generated by the temperature-gradient between two half-cells [1].

As shown in Figure 1, two electrodes are immersed in an electrolyte at regions which differ in temperature. Temperature differences are obtained by heating one half-cell and cooling the other. An electrical circuit is connected to the electrodes to allow for removal of electrical energy from the cell. During the passage of current through the cell, matter is transferred from one electrode to the other as a result of the electrochemical reaction at the electrode/electrolyte interface and ionic transport in the electrolyte. In the copper sulfate solution the high temperature copper electrode is the cathode and the low temperature copper electrode is the anode [6]. In this respect the thermogalvanic cell differs from metallic thermocouples, or thermoelectric devices in general, in which no net transfer of materials occurs, and the state of the conductor remains unchanged with the passage of current.

The potential difference between both half-cell potentials taken at open-circuit corresponds to thermodynamic equilibrium and is defined as:

$$E_{oc} = \phi_0(II) - \phi_0(I) \tag{1}$$

ϕ_0, the potential of one half-cell, is due to the potential difference at the electrode-electrolyte interface,

$$\phi_0 = \phi_{00} + \frac{R \cdot T_0}{z \cdot F} \cdot \ln a_{Me^{z+}} \tag{2}$$

where, ϕ_{00} = standard electrode potential, R = molar gas constant, T_0 = absolute temperature, z = number of charges of the ion, F = Faraday's constant and a_{Mez+} the activity of the metal ion.

When the temperature of half-cell (II) is raised to the temperature $\underline{T = T_0 + \Delta T}$, the potential of this half-cell is changed to

$$\phi_0(II) = \phi_0(I) + \frac{d\phi_0}{dT} \cdot \Delta T \tag{3}$$

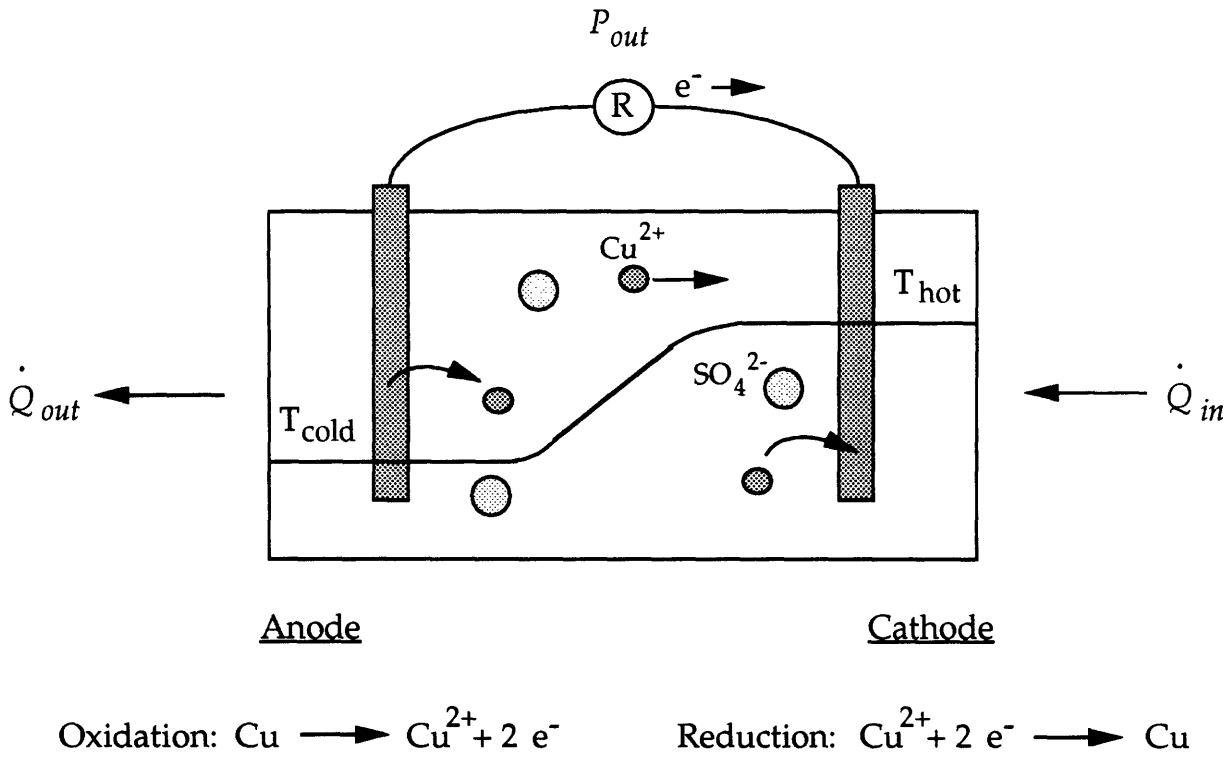

Figure 1: Principle of Operation Using $CuSO_4$ as Electrolyte

where,

$$\frac{d\phi_0}{dT} = \frac{d\phi_{00}}{dT} + \frac{R}{z \cdot F} \cdot \ln a_{Me^{z+}} + \frac{R \cdot T_0}{z \cdot F} \cdot \frac{d \ln a_{Me^{z+}}}{dT} \qquad (4)$$

is the thermoelectric power. When combined with Equation (1), this leads to the definition of the thermogalvanic emf:

$$E_{oc} = \frac{d\phi_0}{dT} \cdot \Delta T \qquad (5)$$

By analogy with thermoelectric phenomena, the gradient $\underline{d\phi_0/dT}$ in Equation (5) is defined as the Seebeck-coefficient (S). Thus Equation (5) can be written as

$$E_{oc} = S \cdot \Delta T \qquad (6)$$

2.2 CELL PERFORMANCE

When evaluating the power generating abilities of thermogalvanic cells, it is best to make direct measurements of the current output. This is achieved by placing a variable external load resistance, R_{ext}, into the circuit and measuring the cell potential.

Figure 2 shows the result of one experiment. The current (I) and the power-output (P) are calculated with the following Ohm's law relationships:

$$I = \frac{E}{R_{ext}} \qquad (7)$$

$$P = E \cdot I = \frac{E^2}{R_{ext}} \qquad (8)$$

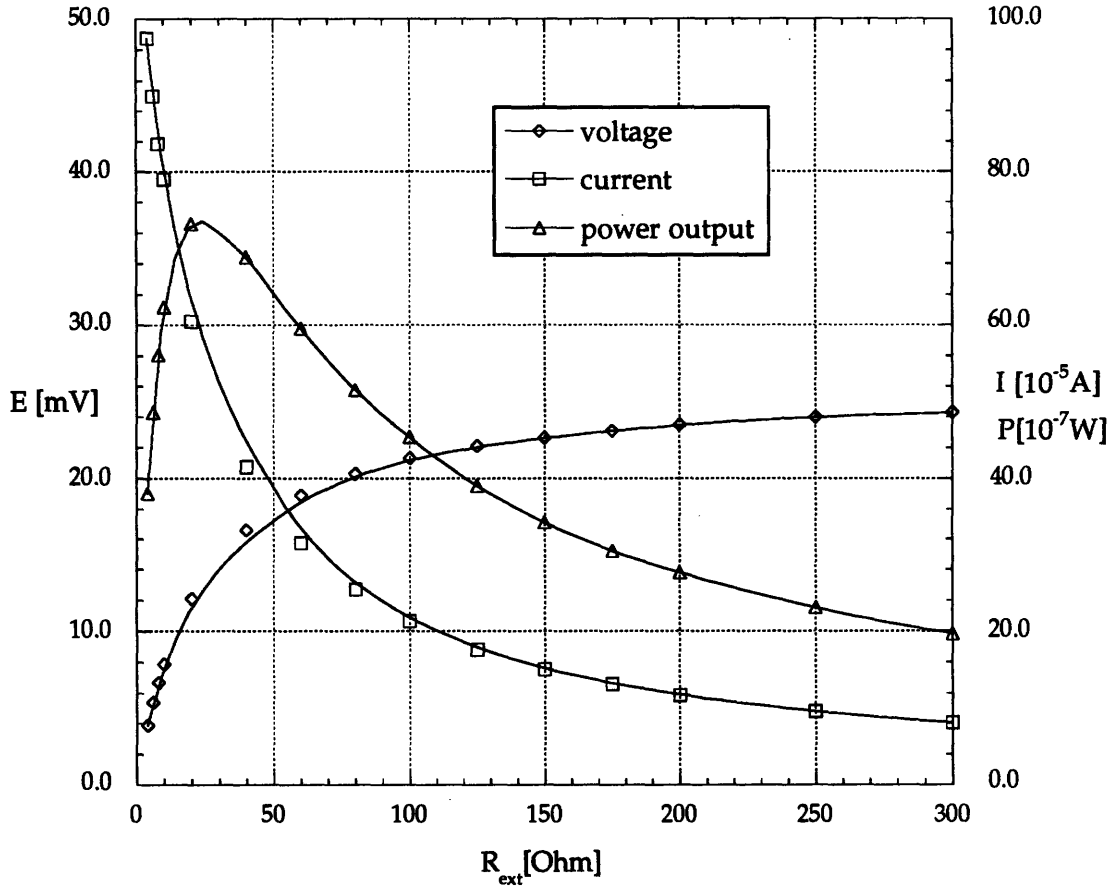

Figure 2: Cell Performance: Cell Type I, 15 wt% $CuSO_4$, T_h-T_c = 39 °C

The maximum power-output, P_{max} , is determined from the maximum of the graph of P against R_{ext}.

2.3 VOLTAGE-CURRENT CURVES

A more convenient way to obtain P_{max} uses voltage-current (E-I) curves. Figure 3 shows the E-I curve plotted from the data given in Figure 2. For linear E-I curves, the internal resistance of the cell, R_{int}, is equal to the external resistance at $E = 1/2\ E_{oc}$. At this point the power-output is a maximum as given by the rectangle of the area under the E-I curve in Figure 3:

$$P_{max} = \frac{E_{oc}}{2} \cdot I\,(\text{at } E = E_{oc}/2) = \frac{E_{oc}^2}{4 \cdot R_{int}} \qquad (9)$$

When the E-I curves of thermogalvanic cells are linear, P_{max} and R_{int} can be calculated with only one value for the voltage measured at an specific external resistance and the open circuit voltage:

$$R_{int} = \frac{E_{oc}}{E} \cdot R_{ext} - R_{ext} \qquad (10)$$

The open-circuit cell potential is expressed by $\underline{S \cdot \Delta T}$, which leads to:

$$P_{max} = \frac{S^2 \cdot \Delta T^2}{4 \cdot R_{int}} \qquad (11)$$

The advantage of using the E-I curve is that it directly shows the two important variables determining power-output: E_{oc} and R_{int}.

2.4 POWER CONVERSION EFFICIENCY

The thermodynamic conversion efficiency, η, of a non-isothermal cell is defined as follows [7]:

$$\eta \equiv \frac{\text{electrical power output}}{\text{thermal power flowing through the cell}} = \frac{P_{max}}{\dot{Q}} \qquad (12)$$

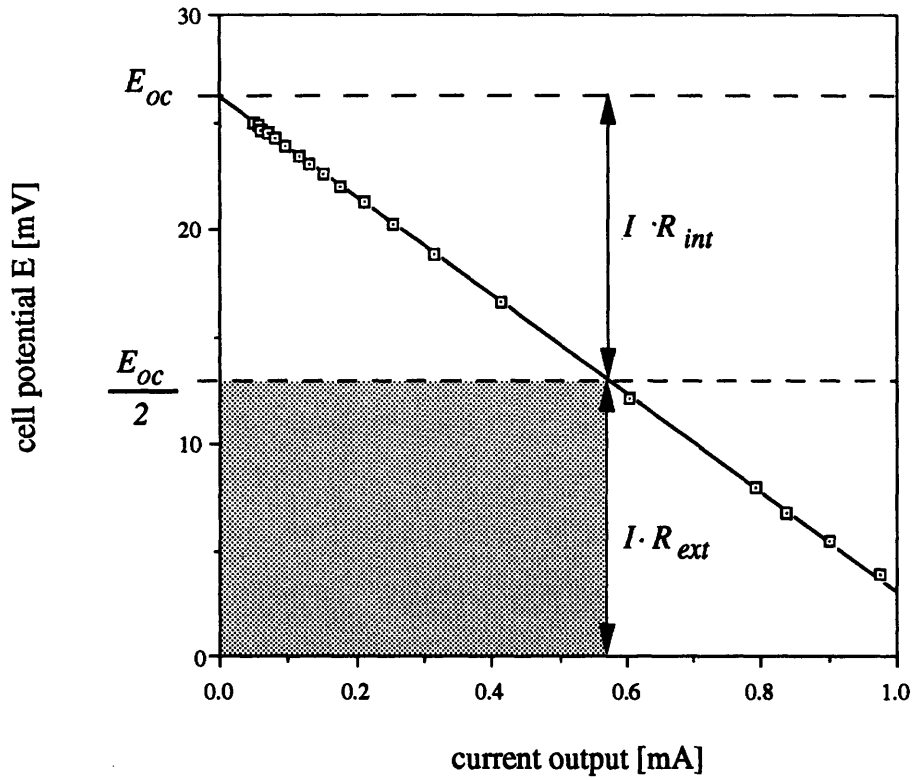

Figure 3: Characteristic E-I Curve

The electrical power output is commonly expressed as the maximum value, P_{max}. The thermal power flowing through the cell consists of two parts: the rate of heat transmission due to simple thermal conduction and the rate of heat transfer through the cell due to the reversible heat of the cell reaction.

Since in our case no net cell exists, Equation (12) can be written as:

$$\eta \simeq \frac{P_{max}}{k \cdot A \cdot \frac{dT}{dx}} \qquad (13)$$

where k is the thermal conductivity of the electrolyte, A is the cross sectional area of the cell and dT/dx is the temperature gradient with respect to x, the distance between the electrodes.

3. EXPERIMENTAL STUDIES

3.1 CELL CHARACTERISTICS

Experiments were carried out with two different types of cells. The cylindrical body of the cells (d_i = 4.3 cm, d_o = 7.5 cm) was constructed from polysulfone and removable sections are clamped into position. A heated magnetic stirrer supplies heat. Cooling is facilitated by a thermostat. The cell is connected to a load resistance designated as R and the electrical potential difference between the electrodes is measured with a digital voltmeter (Escort EDM 1111A) and recorded with a recorder (HP 7132A). Figure 4 shows schematics of the types of cells used in our study.

In cell type I the driving temperature difference is obtained by cooling the electrolyte on one side and heating the electrolyte on the other side. The electrolytes are pumped through the cell which is divided into two parts by an electropermeable membrane (EPM) supplied from the T and G Corporation. The membrane serves as a thermal barrier between half-cells which prevents the hot and cold electrolytes from mixing and over which the temperature gradient occurs. Figure 4 qualitatively shows the temperature profile within each cell configuration. The greatest temperature

gradient occurs in a small area around the membrane. On each side Cu-electrodes (99.99%, 30 mm length, 13 mm width) are immersed in the electrolyte. The temperature in each half-cell is measured with a thermocouple to an accuracy of 0.1°C.

As opposed to cell type I, the electrolyte in cell type II is not circulated. In this case the electrodes act as walls confining the electrolyte. The temperature difference is maintained by pumping heated and cooled water through the outer cell sections. In this cell type the temperature gradient is approximately constant and is equal to the temperature difference divided by the distance between the hot and cold electrode.

3.2 EXPERIMENTAL PROCEDURES

The electrolyte solutions used were prepared using the following salts dissolved in deionized water: $CuSO_4 \cdot 5H_2O$ (Mallinckrodt, Inc.), Cu(II)-acetate (Johnson Matthey Electronics) and $CuClO_4$ (Johnson Matthey Electronics) both with greater than 99% purity. At the onset of each experiment, copper electrodes were rinsed with distilled water, polished with sandpaper then rinsed again and dried. Electrodes were used immediately after treatment.

After assembling the cell, the electrolyte was added and the cell was connected to the voltage recorder. A thermostat regulated the cold half-cell temperature, while a magnetic stirrer slowly increased the temperature of the hot half-cell in stepwise increments. After reaching thermal and electrochemical steady state ($\Delta T \rightarrow$ constant, $E_{oc} \rightarrow$ constant) temperatures and voltages were measured and the heated half-cell temperature was increased. After 4 to 5 hours, the last open circuit value could be measured and the cell was then connected to a variable resistance load. Voltages were then measured for different resistances, always allowing the cell to reach equilibrium.

Measured open circuit values were plotted on an E_{oc} versus ΔT graph in order to obtain the Seebeck-coefficient. Points were fitted linearly and the slope of this line was taken as the Seebeck-coefficient, S, (see Equations (5) and (6)).

To calculate the voltage-current characteristic curve, the current output, I, was calculated with Equation (7) and plotted against the measured, corresponding closed circuit data for the cell potential. The negative slope of the resulting line indicated the internal resistance, R_{int}, (see Figure 3). The maximum power output, P_{max}, was calculated using Equation (11) and the measured values of S and R_{int}.

4. RESULTS AND DISCUSSION

4.1 EFFECT OF ELECTROLYTE CONCENTRATION ON CELL PERFORMANCE

A variety of systems, using cells shown in Figure 4, were used in determining Seebeck-coefficients and internal resistances. The $CuSO_4$ system was chosen to verify the dependence of the Seebeck-coefficient and the internal resistance on the electrolyte concentration, and therefore on the power generating ability of the cells.

Concentration Dependence of Seebeck-Coefficient: Figure 5 shows the result of the experiments evaluating the concentration dependence of the Seebeck-coefficient. $CuSO_4$-concentrations were varied from 0.05 wt% to 5 wt% and the temperature difference was varied from 3°C to 57°C. The graph shows typical results of experimental measurements of Seebeck-coefficients in thermogalvanic cells in this temperature range. The linear relation is observed for all concentrations.

The open circuit cell potential was measured in reference to the high-temperature electrode. The Seebeck coefficients are positive meaning that the electric potential of the high-temperature electrode is positive with respect to that of the low-temperature one. Therefore, the hot electrode is the cathode.

As can be seen by the different slopes in Figure 5, the electric potential difference per unit temperature difference depends on the concentration. The Seebeck coefficient increases with decreasing electrolyte concentration.

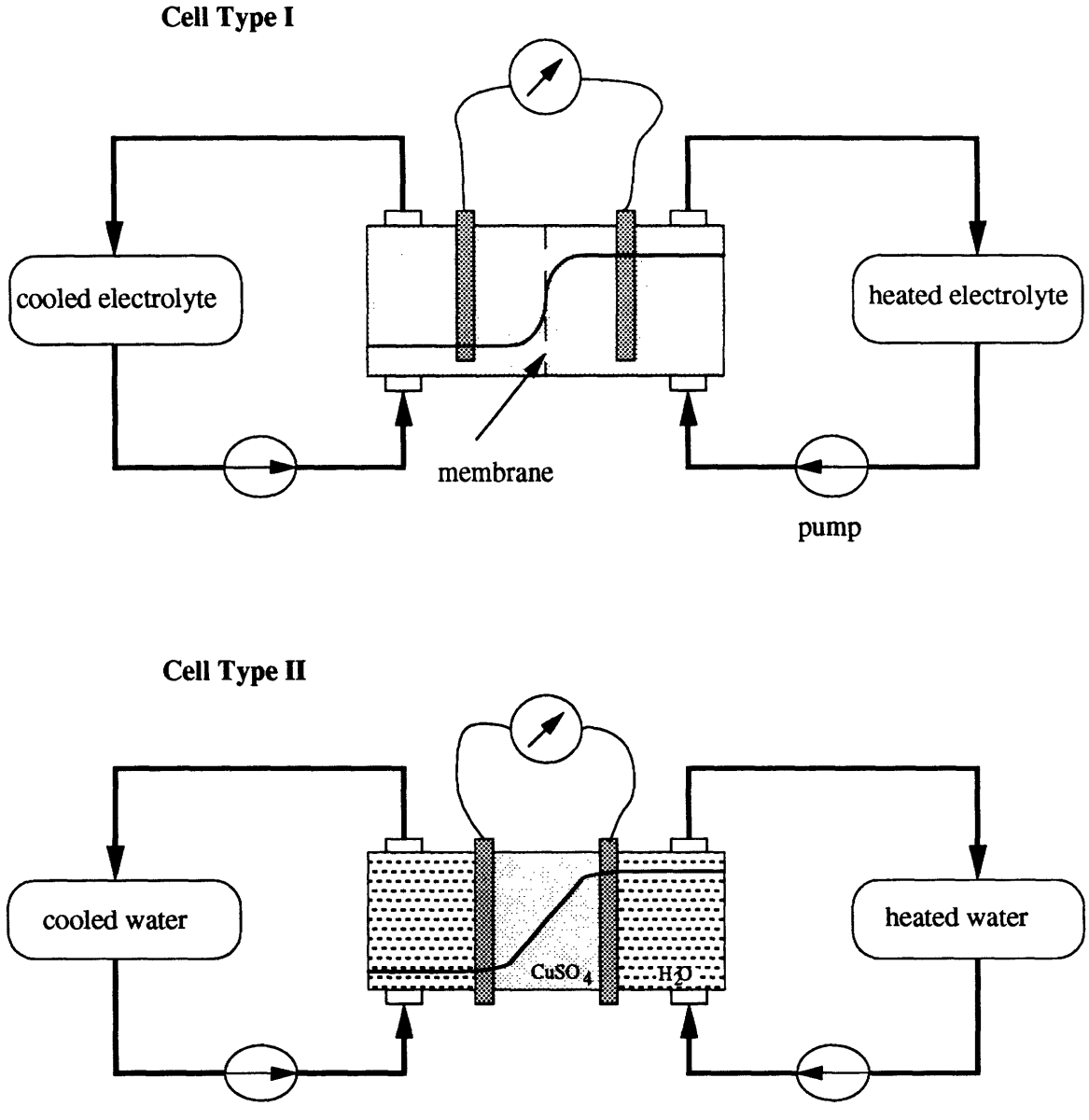

Figure 4: Flowsheets of Cell Types I and II

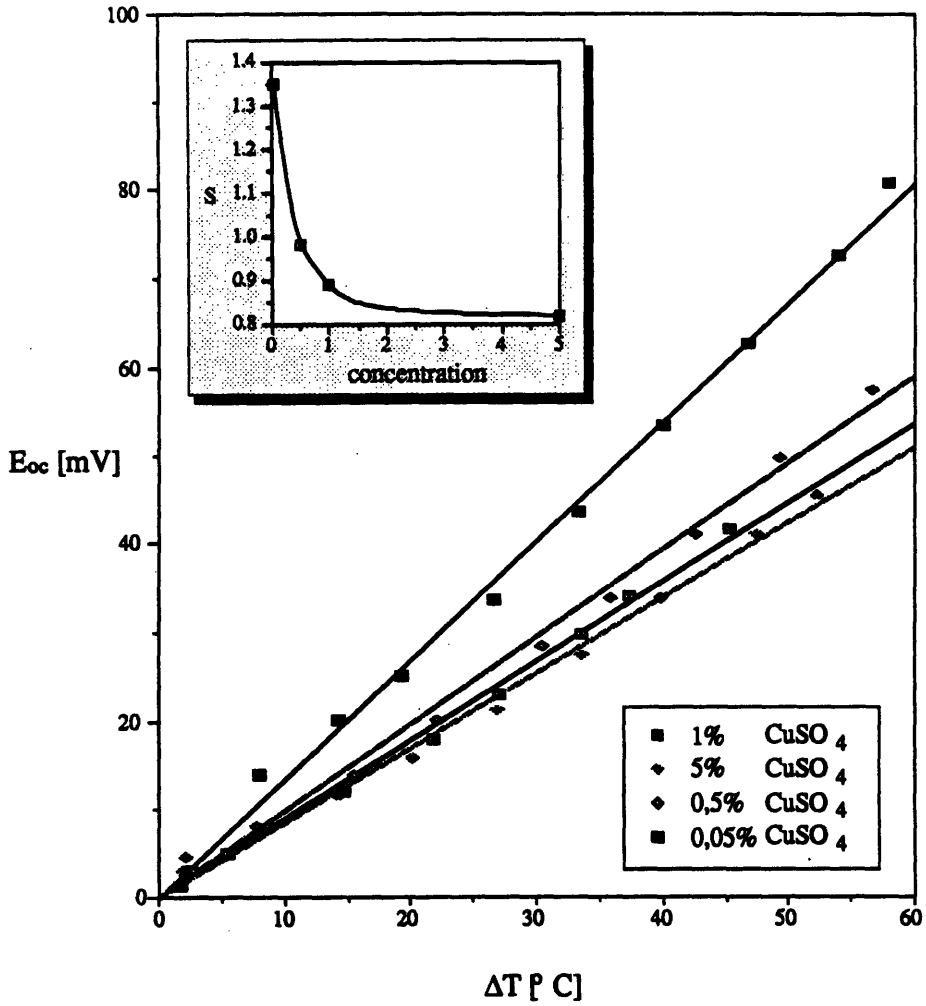

Figure 5: Concentration Dependence of Seebeck-Coefficient

To fit the lines to the origin, the open circuit cell potential on the vertical axis is corrected. Actually, these lines are displaced slightly due to the effect of asymmetry potentials which exist across any thermocell when $\Delta T = 0$, because of small differences in the individual electrodes [10].

Concentration Dependence of Internal Resistance: To evaluate the power generating abilities of thermogalvanic cells, it is best to use the voltage-current characteristic curve. This curve directly shows the value of the internal resistance, R_{int}, as well as the maximum power output.

To verify the concentration dependence on the internal resistance and therefore on the maximum power output, the concentration of $CuSO_4$-electrolyte was varied between 0.5 wt% and 15 wt%. Temperature differences for each experiment were chosen so that the open circuit voltages was approximately 26.5 mV. Figure 6 shows the results. The linear relation between E and I can be observed clearly for all concentrations. The internal resistance (equal to the negative slope of E-I curves) increases considerably with increasing degree of dilution. For high concentrations, the influence is not significant so that beyond a certain limit an additional increase of the electrolyte concentration does not significantly affect the internal resistance. The decrease of R_{int} for high concentrations can be explained with the increasing of electrolyte conductivity due to the higher density of ions and their ability to carry charges.

Concentration Dependence of Maximum Power Output: Figure 7 shows the concentration dependence of the Seebeck coefficient, the concentration dependence of R_{int}, and the resulting effect on the maximum power output. The maximum power output, P_{max}, is calculated with Equation (11) from the voltage-current characteristic curve.

Although Seebeck coefficients (S) are high at low concentrations, the power output is low due to high internal resistance at low concentrations. With increasing concentration, R_{int} decreases. This increases the maximum power output because decrease in S with increasing concentration is proportionally less

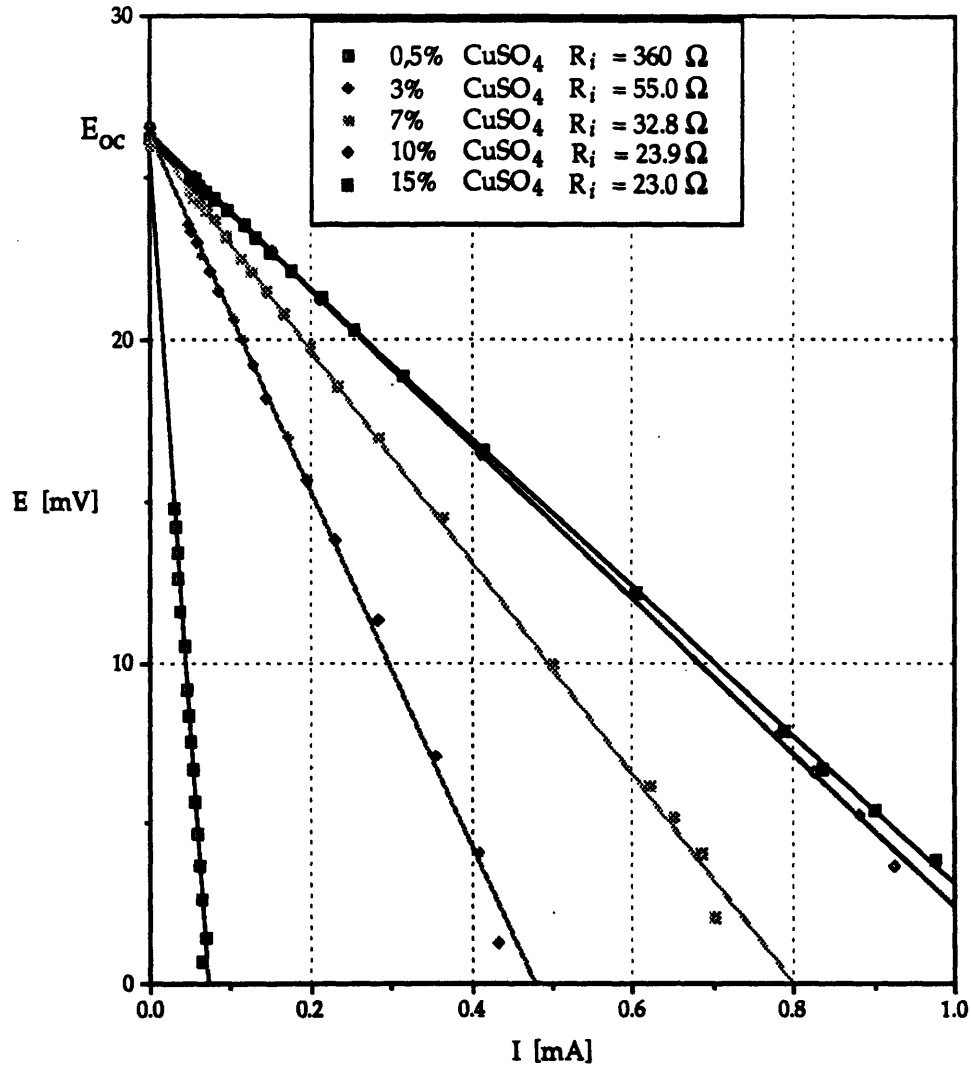

Figure 6: Concentration Dependence of Internal Resistance, Cell Type I

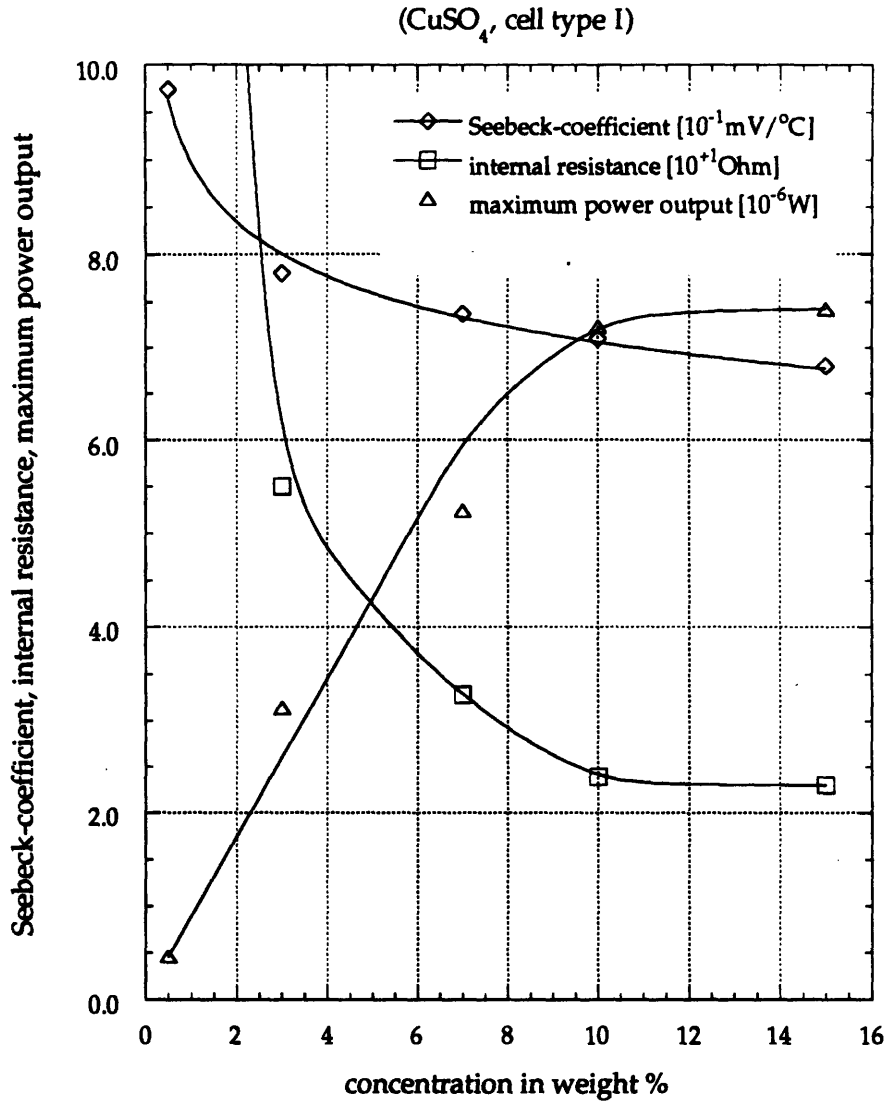

Figure 7: Dependence of Seebeck-coefficient, Internal Resistance and Maximum Power Output on $CuSO_4$ Concentration

than the decrease of R_{int}. P_{max} increases until leveling off around 10 wt% $CuSO_4$.

4.2 INFLUENCE OF MEMBRANE ON INTERNAL RESISTANCE

The internal resistance of the thermogalvanic cell is derived from several parts: the resistance of the electrolyte, the resistance of electrodes, the resistance of the wires and junctions, the electrode/electrolyte interface resistance and the resistance of the separator (which serves as a thermal barrier in cell type I). In this section, we will focus on the internal resistance of the cell's internal separator.

Two different membranes (labelled 2500 and 1225) and a glass frit were used in our tests. The membranes, supplied by T and G Corporation are according to Peck "nonporous and electropermeable". They consist of a supporting sheet covered with an ionic semiconductive material, which consists of long-chain hydrogel molecules dispersed and bound within a nonporous chemically resistant plastic matrix [4]. The membranes are made in a range of ionic conductances by changing the composition. The glass frit used was a sintered glass filter disc with a thickness of 4 mm and a porosity of 41 μm.

Figure 8 shows the results for a 5 wt% $CuSO_4$-electrolyte using the different separators. The differences in internal resistances are evident. The greatest value occurs in the cell with the 1225 membrane. Here R_{int} is about 132 Ω. Even the cell with the glass frit has a lower resistance, about 71 Ω. The best separator seems to be the 2500 membrane. Here, the internal cell resistance is about 29 Ω, which is on the same order as the internal resistance of a type II cell using the same electrolyte, but without any separator. This means that the membrane 2500 is an excellent separator in a galvanic cell, with a minimal additional resistance.

Although the 2500 membrane has a minimal additional resistance, the internal cell resistance shows an influence from the membrane area. For example: with decreasing membrane area from 14.5 cm^2 to 7.25 cm^2, the internal resistance of a cell using a 3 wt% $CuSO_4$-electrolyte increased from 22.7 Ω to 28.1 Ω.

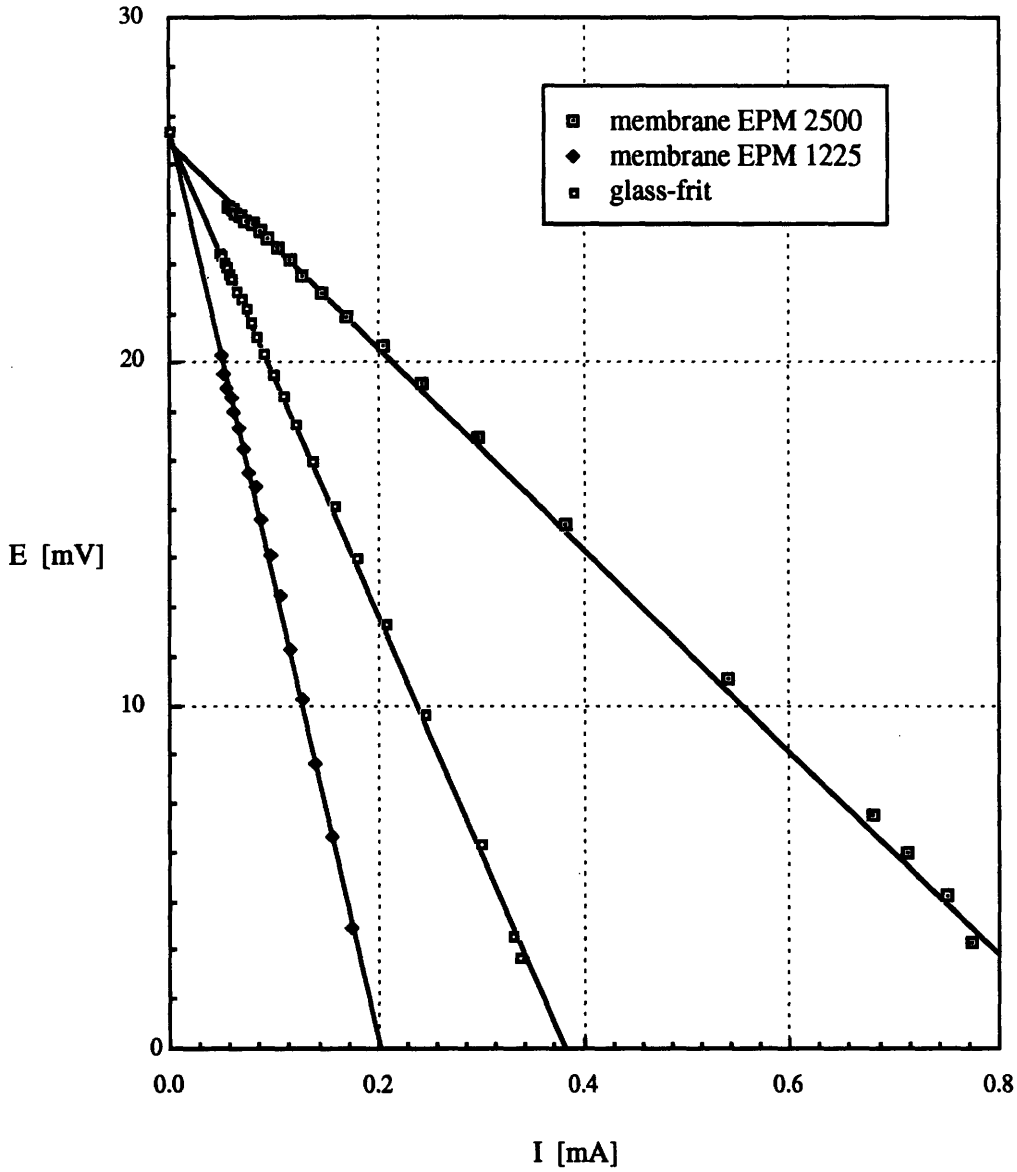

Figure 8: Influence of Separator on Internal Resistance

The membrane resistance is not only a function of the chemical composition of the used semiconductive material, but also a function of the operating time. For example, the internal resistance of a cell using 3 wt% $CuSO_4$ electrolyte and the 2500 membrane, increased by 20 % after 27 hours of total operating time.

4.3 VARIATION OF GEOMETRY AND ITS INFLUENCE ON THE INTERNAL RESISTANCE

As pointed out in the preceding section, internal resistances of thermogalvanic cells may be divided into several components: 1. the resistances of the electrodes which are associated with the nature of the supporting anode and cathode electrode structure, 2. the electrolyte resistance, R_e, which is determined by the ionic concentration of the cell electrolyte, 3. the separator resistance and 4. the "resistances" of the electrode/electrolyte interfaces. These last "resistances" are actually impedances, because they behave not like real ohmic resistances. The nature of these impedances depends on the specific nature and condition of the reactions at the electrode surface.

To evaluate the influence of the electrode/electrolyte interface impedance on the internal resistance of the cell, the electrode area was changed. This change did not influence the internal resistance of the cell (10 wt% $CuSO_4$, cell type I, ΔT = 60°C). Even a doubling of the electrode surface from 7.8 cm^2 to 15.4 cm^2 did not change the value of R_{int}.

In section 4.1, we discussed the strong influence of the electrolyte concentration on the internal cell resistance. This suggests that the internal resistance is also a function of electrode-distance. To evaluate these dependencies, a cell was constructed which permitted variation of the electrode-distance from 1 to 4 cm.

Figures 9 and 10 show the results for 3 wt%- and 15 wt% $CuSO_4$-electrolyte. The internal resistance increases with increasing electrode distance. For high concentrations, the influence is not significant. For low concentrations, however, the internal resistance is a strong function of electrode separation. This

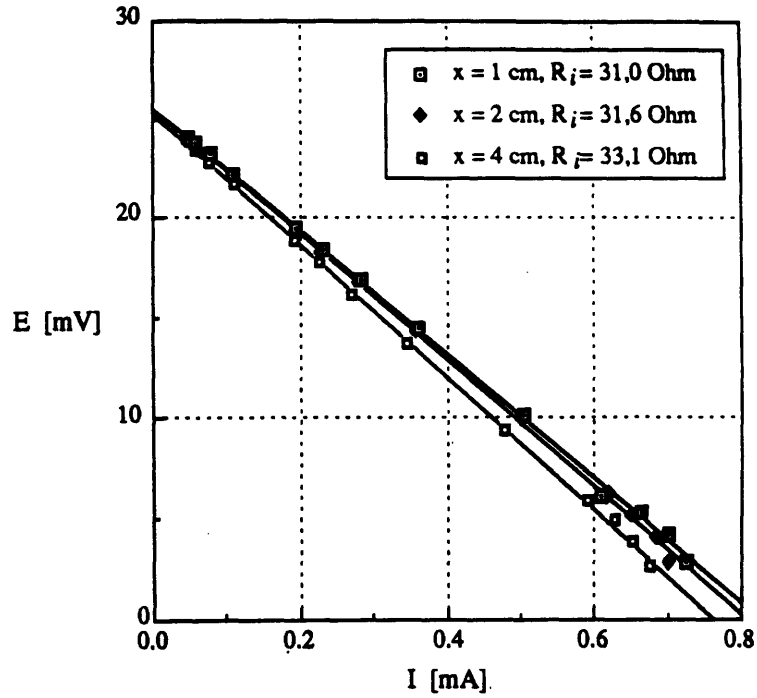

Figure 9: Influence of Electrode Distance, Cell Type I, 3wt% $CuSO_4$

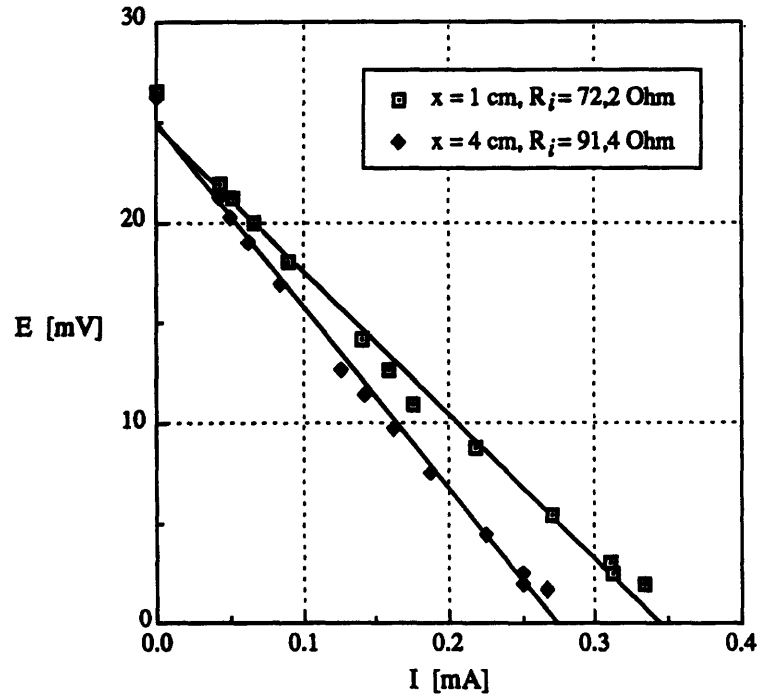

Figure 10: Influence of Electrode Distance, Cell Type I, 15 wt% $CuSO_4$

behavior is coupled with the inherent concentration dependence of R_{int} on the electrolyte concentration. In practice, R_{int} is largely limited by the ohmic resistance of the electrolyte.

4.4 EFFICIENCIES

Two different cell types were used in our experiments. Power conversion efficiencies were calculated using Equation (12). Table 1 shows the results for a 10 wt% $CuSO_4$-electrolyte.

Cell Type	ΔT [°C]	η [%]
I	59.8	0.000025
II	68.15	0.000425

Table 1: Power conversion efficiencies for cell type I and cell type II.

The power conversion efficiencies of thermogalvanic cells are very small. The efficiency of cell type II is approximately 20 times higher than the efficiency of cell type I. This is due to the high temperature gradient in cell type I which causes significant heat flow through the cell (section 3.1). In cell type II, the temperature gradient is a linear function of the electrode distance and is therefore smaller than in cell type I. In practice, with maximum power from the cell, varying the separation of the electrodes does not change power significantly, while it does change thermal conductance and hence the efficiency of thermogalvanic cells. Therefore, the best cell should be a cell type II with a relatively high electrode separation (in the order of centimeters).

4.5 EFFORTS TO ENHANCE PERFORMANCE

The power efficiency of a thermogalvanic cell is proportional to the heat conduction through the electrolyte. If, for example, the electrodes are located closely together so that the internal

electrical conductance is raised, the electrical power output is increased. However, by positioning the electrodes closely together, heat conduction is also increased. The resulting heat flow causes a decrease in the power efficiency.

The power efficiency of thermogalvanic cells can be increased by reducing the thermal conductivity by use of thermal barriers. Thermal barrier materials are additives to the electrolyte system such as silica gel or powdered silica. Table 2 shows the results for some examples of electrolytes and electrolyte silica mixtures. The silica used was Cab-O-Sil®, a form of fumed silica manufactured by Cabot (Grade M 5).

Electrolyte	T_m [°C]	S [mV/°C]	R_i [Ω]	P_{max} [μW]	η [%]
10% $CuSO_4$	54.38	0.70	23.6	25.3	0.00043
10% $CuSO_4$ +7% Cab-O-Sil	60.10	0.89	12.2	95.0	0.0074
41.85% $Cu(ClO_4)2$ +7% Cab-O-Sil	59.15	1.09	1.84	1000	0.08
7%Cu(II)Acetate	44.40	1.36	18.3	60.3	0.0015

Table 2: Power conversion efficiencies.

Three effects can be observed when the salt is complexed with a 7 wt% Cab-O-Sil®: 1. increased Seebeck-coefficient, 2. decreased internal resistance, and 3. decreased thermal conductivity.

The best salt tested is the Cu(II)-perchlorate. The efficiency of the copper perchlorate + Cab-O-Sil® cell is calculated to be 0.08 % and is therefore about 200 times higher than the efficiency of a cell using a simple $CuSO_4$-electrolyte. With a Seebeck-coefficient of 1.09 mV/°C and a internal resistance of 1.84 Ω the cell could produce a maximum power of 1 mW.

Another very interesting aspect of using silica were the long-term effects on the Seebeck coefficient. Figure 11 shows the Seebeck coefficient over a period of more than 4 months. As given

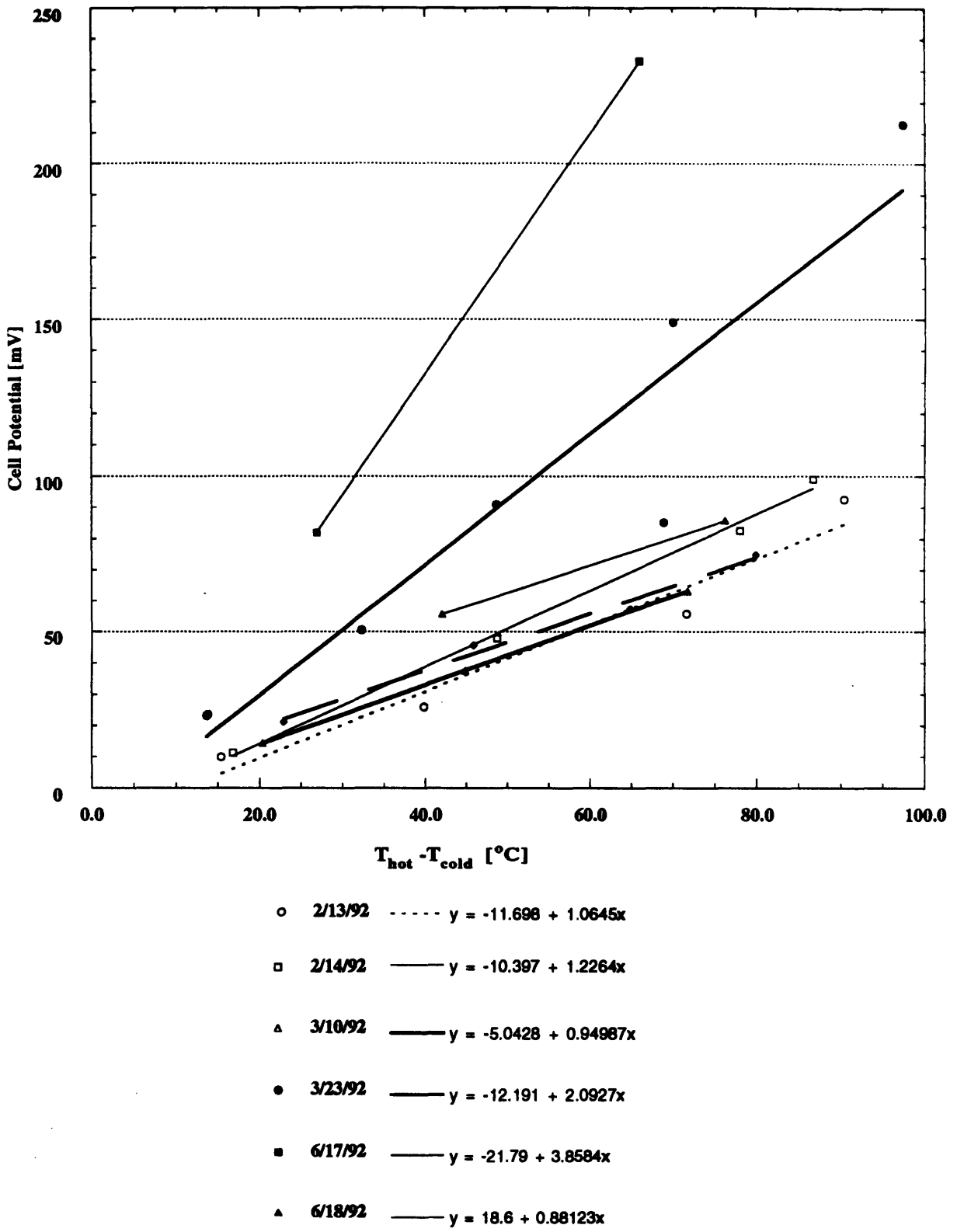

Figure 11: Open Circuit Cell Potential versus Temperature Difference. The Seebeck coefficient is given by the slope of each line. Least squares equations are also shown where, y = cell potential, x = ΔT

by the slopes in Figure 11, the Seebeck coefficient increased from 1.06 mV/°C on 2/13/92 to 3.86 on 6/17/92. This surprising almost fourfold increase indicates a change in the structure of the electrolyte requiring long periods of time. This increase of S is very desirable because P_{max} rises quadratically with S as can be seen from Equation (11). We therefore connected a load to the cell to measure P, right after the high S was measured. Disappointingly, we measured about the same P than in the previous experiments suggesting that the rise in S was accompanied by an increase in R_{int}. In terms of P in Equation (11), these effects seem to cancel each other resulting in no net increase of P.

After measuring P of the cell, we remeasured S to find that S returned to "normal levels" as shown in Figure 11 by the data generated during runs on 6/18/92 and 6/30/92. This suggests that the transport of ions through the electrolyte has destroyed the structure which caused the observed increase in S.

5. CONCLUSIONS

Our research has shown that the two cell types used are technically feasible systems to convert thermal to electrical energy. The best cell in terms of power density and efficiency used copper perchlorate with silica. It delivered up to 0.07 mW/cm^2 with a temperature gradient of 59°C at a efficiency of about 0.08%. These numbers represent a significant improvement compared to cells using pure electrolyte as investigated at the outset of this project. However, the observed power densities and efficiencies are at least one order of magnitude too low to make the systems economically viable based on a report written by D.J. Curtin [11]. Curtin calculated the approximate cost of electrical energy generated by thermogalvanic converters with a rated power output of 20 KW and 1 MW. To compare costs, he also evaluated conventional generators fueled by diesel, oil and coal. The results show that electrical power generated by thermogalvanic cells was at least twice as expensive than generated by conventional means. Curtin assumed a cell output of 2.8 W/ft^2 which corresponds to 3 mW/cm^2. This value is more than forty times higher than the maximal power output achieved in this project. Furthermore, Curtin assumed efficiencies of 2%, which is more than twenty times as high than the values measured in this project. Taking into account these discrepancies, our results seem to indicate that thermogalvanic cells are even less competitive than the Curtin analysis concluded.

Peck has reported that higher power densities were obtained by using temperature gradients along the electrodes. We have conducted a number of experiments with electrode temperature gradients with as setup that closely resembling Peck's. However, we did not observe any improvements. We discussed our results extensively with Mr. Peck to find possible explanations and further changes in the setup were considered. At the present time, the discrepancies between the data could not be resolved.

In conclusion, we were able to reproduce some of Peck's work. Clearly, the addition of silica decreases the internal resistance considerably, this by itself being a major achievement. Mr. Peck

has also mentioned that he has observed increased Seebeck coefficients although these results were not reproducible. As discussed in the preceding section, we observed a surprising increase in the Seebeck coefficient over a period of three months. However, when measuring power output, we found that the increase in the Seebeck coefficient was accompanied by an increase of the internal resistance which compensated for the increase of the Seebeck coefficient. Thus the measured power output remained about the same. Clearly, the combined effects of Seebeck coefficient and internal resistance variations have to be taken into account when evaluating cell performance.

6. RECOMMENDATIONS

We believe that optimization of the systems investigated in this project can improve efficiencies from 0.1% to 1.0% and the power densities from 0.07 mW to 0.5 mW. However, major breakthroughs are required to allow commercialization of this technology. Based on the Curtin report, we think a commercially attractive system would require efficiencies of about 5% and power densities of 30 mW. Another factor only marginally addressed in this study is long-term behavior of the system. Likely problem areas are uneven plating on the electrodes and corrosion. Another issue to be addressed is the series connection of single cells. Since a single cell only yields a voltage of less than 0.1 V, at least 400 of cells have to be connected in series to reach around 40 V, the voltage necessary to allow efficient conversion from DC to AC.

Further progress will require a considerable effort. Key research issues involve screening of electrolytes and additives on a trial and error basis to maximize system performance.

7. ACKNOWLEDGEMENTS

We would like to thank Crucible Ventures for funding this project. Sincere appreciation goes to Robert Peck and Adrian Horne for their help, patience and advice.

8. REFERENCES

[1] Agar, J. N., Thermogalvanic Cells, in Advances in Electrochemistry and Electrochemical Engineering, Delahay, P. and Tobias, C. W., eds., vol.3, (1963).

[2] Christy, R. W., Ch.12 in Cadoff, I. B. and Miller, E., eds., Thermoelectric Materials and Devices, Reinhold, New York, (1960).

[3] Sundheim, B. R., Ch.14 in Cadoff, I. B. and Miller, E., eds., Thermoelectric Materials and Devices, Reinhold, New York, (1960).

[4] Peck, R. L., Ionic Semiconductor Materials and Applications Thereof, United States Patent # 4,797,190, Jan. 10, 1989.

[5] Peck, R. L., Thermoelectric Energy System, United States Patent #4,211,828, Nov. 9, 1978.

[6] Uhlig, H. H. and Revie, R. W., Corrosion and Corrosion Control, John Wiley & Sons, Inc., (1985).

[7] Quickenden, T. I. and Vernon, C. F., Thermogalvanic Conversion of Heat to Electricity, Solar Energy, vol. 36, (1986).

[8] Anderson, L. B., Greenberg, S. A. and Adams, G. B., Thermally and Photochemically Regenerative Electrochemical Systems, Ch. 15 in Regenerative EMF Cells, Advances in Chem., vol. 64, (1964).

[9] Richter, J., Heller, A. und Vreuls, W., Untersuchungen an nicht-isothermen Salzschmelzen, Bericht der Bunsenges. Physik. Chem., Bd. 81, Nr. 4, (1977).

[10] Tyrrell, H. J. V., Thermal Diffusion Studies: II. Electrolyte Solutions, Ch. 10 in Diffusion and Heat Flow in Liquids, Butterworth & Co. Ltd., London, (1961).

[11] Curtin D.J., Power Cost Estimates for Kali Cells, internal memorandum ARCO, Dublin Center, April 30, 1980.